Winding Function Model of a 6/7 Variable Flux Reluctance Machine

Seyed Armin Mirnikjoo
Department of Electrical Engineering
K. N. Toosi University of Technology
Tehran, Iran
armin_nikjoo@email.kntu.ac.ir

Karim Abbaszadeh
Department of Electrical Engineering
K. N. Toosi University of Technology
Tehran, Iran

Seyed Ehsan Abdollahi
Electrical and Computer Engineering Department
Babol Noshirvani University of Technology
Babol, Iran

***Abstract*— Variable Flux Reluctance Machine (VFRM) by its doubly salient structure is robust due to the fact that there isn't any windings or Permanent Magnets (PMs) on its rotor structure. Therefore, VFRMs are potential candidates for so many applications including electric vehicles and wind turbines. Consequently, developing a fast and accurate method for its electromagnetic performance analysis is essential. Although Finite Elements Method (FEM) is an accurate method, it is suffering from high simulation time. There are some other methods but they cannot easily apply to all topologies. Winding function is a fast modelling method for analyzing electric machines performance. Therefore, in this paper, Winding function modeling of a VFRM is proposed. In this regard, the concept of VFRMs and winding function modelling procedure is presented. Also, a VFRM which consists of 6 stator teeth and 7 rotor poles number, is modelled by Winding Function Method (WFM) and the results are compared with the experimental results which proves that WFM is an efficient modelling and analysis tool.**

Keywords— variable flux reluctance machine, finite elements method, winding function method, magnetic equivalent circuit, analysis, an imaginary boundary, inductance

I. INTRODUCTION

Variable Flux Reluctance Machine (VFRM) is a reliable and robust electromagnetic system since there is not any windings or Permanent Magnets (PMs) in their rotor structure[1]. Aforementioned feature makes VFRM a suitable candidate for Electric Vehicle (EV) applications [2]. Also, it can be a potential alternative of Permanent Magnet Synchronous Generator (PMSG) and Doubly Fed Induction Generator (DFIG) in wind turbine applications [3-5]. In this regard, developing a fast computing and accurate modeling method, not only leads to an efficient design algorithm, but also a fast and precise optimization tool.

Finite Elements Method (FEM) is employed in so many articles in order to analyze and design of electric machines .In [6] a transversal laminated rotor of a Flux Switching PM motor (FSPM), is designed and analyzed by FEM, however barrier number variation leads to do modeling procedure, again. A brushless three phase Flux Switching Generator (FSG) is proposed in [7]. The proposed FSG is analyzed by FEM, which is enough accurate but it takes a long time for computation and optimization. Consequently, developing another analysis method is essential. In [8] Magnetic Equivalent Circuit (MEC) in which the machine electromagnetic performance is modelled with flux tubes, is used for design procedure of a DC-Excited Flux-Switching Motor (DC-FSM), but applying this method for other geometries requires rebuilding of complicated permeance matrices. In order to analyze electromagnetic performance of a single phase FSPM, a three dimensional Lumped Parameter Method (LPM) is developed. Although the proposed model was enough accurate, it has some intrinsic shortcomings like neglecting winding arrangements [9]. A 12/10 FSPM is modelled by Fourier Analysis (FA) in [10]. Its accuracy was acceptable, but it implies solving complicated fourier equations. Hybrid Analytical Method (HAM) which utilizes MEC and fourier analysis for iron parts and airgap regions, respectively, is proposed in [11] . It suffers from the problems of MEC and fourier analysis. Although these methods are faster than FEM , they do not have enough capability to apply as an efficient modeling method for VFRMs. Winding Function Method (WFM), is another candidate for modeling method of VFRMs design procedure. In [12], [13] the effect of rotor bar and stator skewing is modeled. A Synchronous Reluctance Machine (SyRM) is modelled by FEM and WFM in [14]. WFM has an acceptable inductance computation accuracy. WFM played a key role in optimization procedure of a resolver in [15]. In [16] torque ripple of a Switched Reluctance Machine (SRM) is minimized based on stator teeth and winding appropriated geometries by WFM and 3-dimensional FEM. Also, it is used for inductances computation. In addition, WFM is a popular and robust method for fault diagnostic in electrical machines. In [17] a salient pole synchronous generator with dynamic eccentricity is modeled by WFM. The effect of balanced and unbalanced supply on machine performance is modeled by WFM in [18]. Also, WFM is a potential method for modeling rotor and stator inter turn fault in [19].

This paper, presents an accurate and time-saving WFM modeling of VFRM. In section II the concept of VFRMs is described. Section III illustrates the procedure of WFM modelling. Also, the inductances and torque calculation is investigated in this section. Finally, WFM modelling results are presented and compared with experimental tests in section IV. The comparisons show the accuracy of purposed WFM modeling.

II. CONCEPT OF VFRM

The core structure of rotor and stator of VFRMs are same as Switched Reluctance Machines (SRMs). In addition, DC field winding is located in slots of VFRM as it is shown in Fig. 1. The flux path of VFRMs is different from the flux path of SRMs. Field flux path will change with the rotor rotation. Fig. 2 and Fig. 3 show the variation of flux path among an electrical cycle and the flux line in different positions of rotor, respectively. As it can be seen from Fig. 2, in position A and position C, the airgap reluctance is the minimum value due to the alignment of the stator and rotor teeth while in position B and position D, the rotor teeth is aligned with the stator slots. Thus, the airgap reluctance reaches to its maximum value.

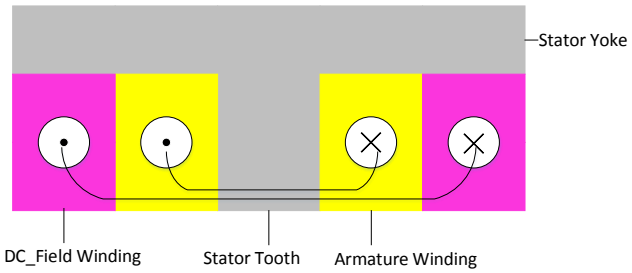

Fig 1: Linear view of VFRM

Therefore, the flux linkage and induced back-EMF in an electric cycle are shown in Fig.4 (a) and Fig.4 (b), respectively. The Ratio of rotor and stator teeth number is a determinant parameter in field flux path, in such a way that field flux can pass through the adjacent stator poles in 6/5 and 6/7 structure. This short flux path can lead to the better performance of machine like lower Total Harmonic Distortion (THD), in comparison with the long one. Windings and their connection are significant factor in VFRMs as individual phase coils should be connected in opposite directions when the number of rotor poles is odd. Fig. 5 shows the vectors of back-EMF in these ratios of rotor and stator teeth number.

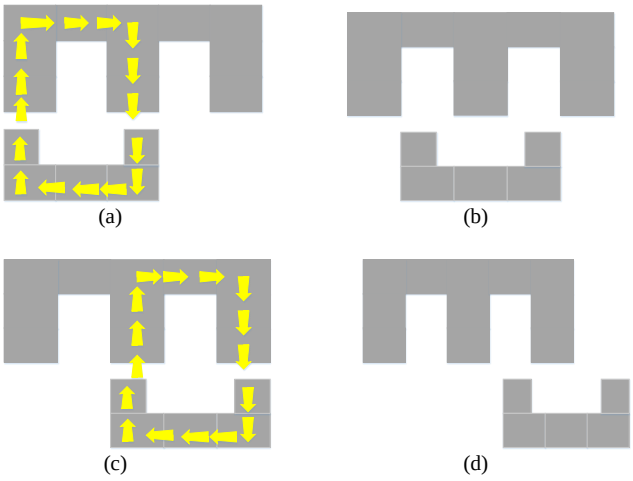

Fig 2: Flux path of VFRM in an electric cycle

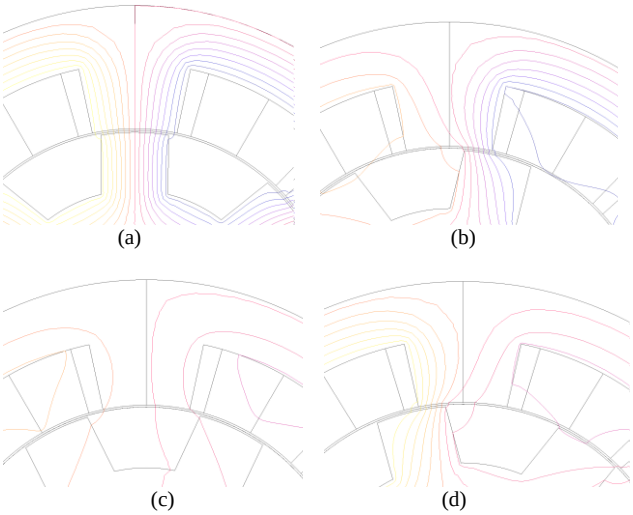

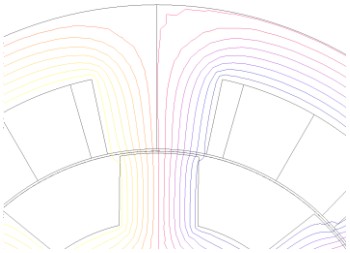

(e)

Fig. 3 : Flux lines among a stator pole of VFRM at 5 different rotor positions

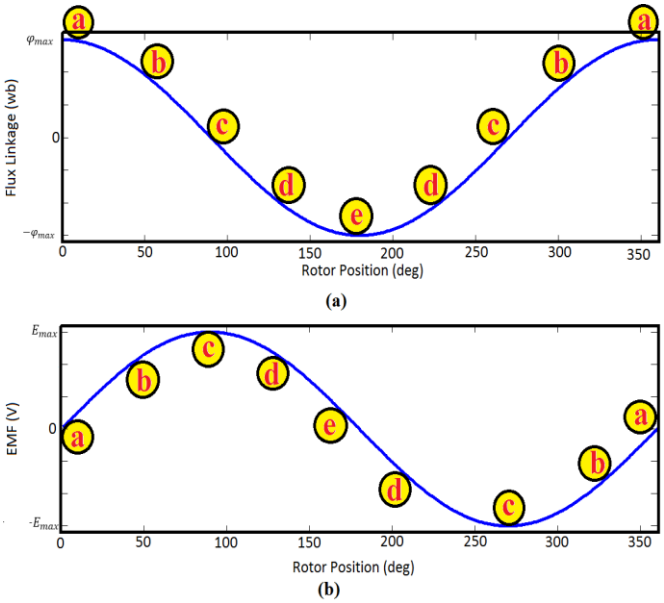

Fig 4: a) Flux linkage among an electric cycle; b) Induced phase voltage among an electric cycle

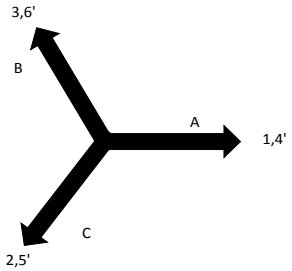

Fig 5 : Phasor diagram of phase coils

III. Winding Function Modeling Procedure Of A 6/7 VFRM

In this section, the basic principal of WFM is going to be introduced. Turn, winding, and airgap function play key roles in winding function modeling of VFRMs.

A. Turn and Winding Function

Turn function proposes the placement of windings among machine geometry. A 2-D cross-section view of a 6/7 VFRM is shown in Fig. 6. The windings of Phase a, phase b, and phase c, are in red, green, and blue, respectively. Also, the DC field windings are in yellow.

.

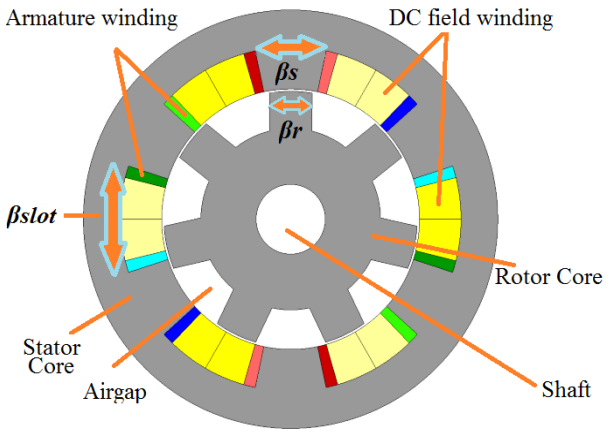

Fig. 6. 2-D cross-section view of a 6/7 VFRM

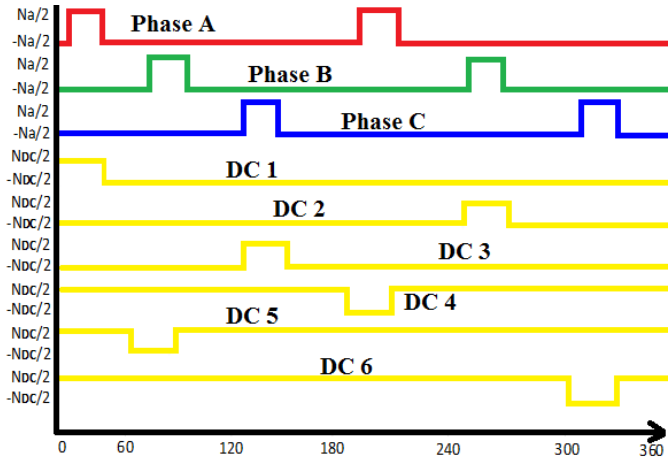

Fig 7: Winding functions

The relation between turn function and winding function is as below:

$$N(\varphi) = n(\varphi) - < n(\varphi) > \quad (1)$$

where $N(\varphi)$, $n(\varphi)$, and $< n(\varphi) >$ are winding function, turn function, and mean of turn function, respectively [20]. The winding functions of abovementioned machine are shown in Fig 7. It is assumed that the upward current flow and downward current flow lead to positive and negative Magneto Motive Force (MMF), respectively.

B. Airgap function

Due to the fact that VFRM is a doubly salient machine, the airgap function is not constant when the rotor rotates. In order to achieve more accurate model, an imaginary boundary has been considered in the middle of the air gap as it is shown in Fig.8. The airgap consists of two functions by this assumption. Fig.9 and Fig.10 show the airgaps which relate to stator and rotor section [21]. According to Fig 9 , the fourier formulation of this air-gap function is given by :

$$G_{sn}(0) = \frac{\beta_s . g_{mins}^{-1} + (\pi - \beta_s) . g_{maxs}^{-1}}{\pi} \quad (2)$$

$$k_{Gs} = \frac{2(g_{mins}^{-1} - g_{maxs}^{-1})}{n\pi} . [\sin\left(\frac{n\beta_s}{2}\right) - \sin(n\pi - \frac{\beta_s}{2})] \quad (3)$$

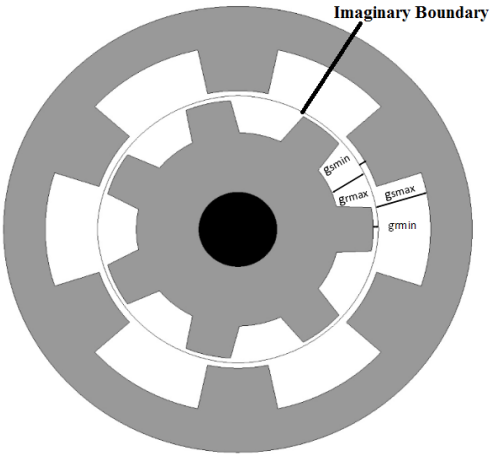

Fig 8: Imaginary boundary in the middle of the air gap of VFRM

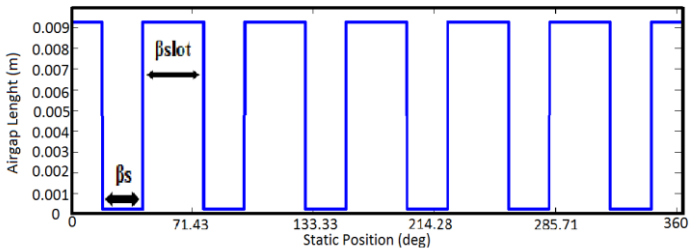

Fig 9: Inverse air-gap function of the stator with reference to imaginary boundary

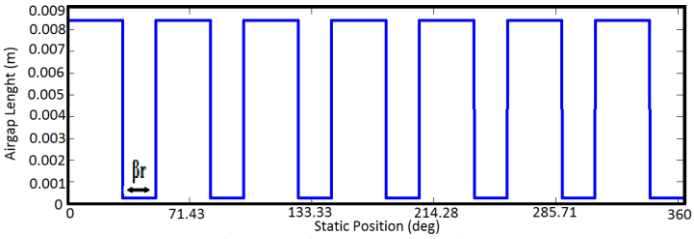

Fig 10: inverse air-gap function of the rotor with reference to imaginary boundary

$$G_s(\varphi) = G_{sn}(0) + \sum_{n=1}^{\infty} k_{Gs} . \cos(n\varphi) \quad (4)$$

where φ, β_s , g_{mins}^{-1}, g_{maxs}^{-1}, and $G_s(\varphi)$ are stator static position, stator pole arc, inverse of the distance from the stator pole face to the imaginary gap-dividing boundary, and inverse of the distance from the inner surface of the back-iron to the imaginary gap-dividing boundary, and fourier series of air-gap function of the stator with reference to imaginary boundary, respectively. The rotation of rotor leads to the variation of air-gap function of the rotor with reference to the imaginary boundary. Hence, this airgap function depends on rotor and stator static position, simultaneously. Also, Fig.10 shows this air-gap function in which, rotor is at zero position. In this regard, fourier series of air-gap function of the rotor with reference to imaginary boundary can be written as (5).

$$G_r(\varphi, \theta) = G_{rn}(0) + \sum_{n=1}^{\infty} k_r . \cos(n(\pi - \theta)) \quad (5)$$

$$G_{rn}(0) = \frac{(2 . \beta_r . g_{minr}^{-1}) + (\pi - 7 . \beta_r) . g_{maxr}^{-1}}{\pi} \quad (6)$$

$$k_r = \frac{2(g_{minr}^{-1} - g_{maxr}^{-1})}{n\pi}.\left[\sin\left(\frac{n\beta_r}{2}\right) - \sin\left(\left(\frac{n\pi}{2}\right) - \left(\frac{n\beta_r}{2}\right)\right) + \sin\left(\left(\frac{n\pi}{2}\right) + \left(\frac{n\beta_r}{2}\right)\right) - \sin\left((n\pi) - \left(\frac{n\beta_r}{2}\right)\right)\right] \quad (7)$$

where θ, β_r, g_{minr}^{-1}, g_{maxr}^{-1}, and $G_r(\varphi,\theta)$ are rotor position, rotor pole arc, inverse of the distance from the rotor pole face to the imaginary gap-dividing boundary, and inverse of the distance from the inner surface of the rotor back-iron to the imaginary gap-dividing boundary, and fourier series of air-gap function of the rotor with reference to imaginary boundary, respectively.

C. Inductance and Torque Calculation

Mutual inductance of two arbitrary windings can be calculated by (8)

$$L_{jk} = \int_0^{2\pi} N_j(\varphi)N_k(\varphi).(G_s(\varphi) + G_r(\varphi,\theta))^{-1}d\varphi \quad (8)$$

where $N_i(\varphi)$ and $N_j(\varphi)$ are winding function of j and k winding. Also, the self-inductance of each winding is as (9).

$$L_{jj} = \int_0^{2\pi} N_j(\varphi)^2.(G_s(\varphi) + G_r(\varphi,\theta))^{-1}d\varphi \quad (9)$$

VFRM follows the elementary principle of electromechanical conversion. Consequently, torque is the ratio of co-energy and rotor position variations, which is depicted in (10)

$$T_e = \frac{\Delta w_f'}{\Delta\theta} \quad (10)$$

Also, the co-energy can be calculated by :

$$w_f' = \frac{1}{2}L(\theta,i).i^2 \quad (11)$$

where $L(\theta,i)$ is the inductance of windings at a particular position θ, and i is the phase current. Therefore, substitution of (11) into (10), leads to the electromagnetic torque equation which is investigated in (12).

$$T_e = \frac{i^2}{2}\frac{dL}{d\theta} \quad (12)$$

Also, $L(\theta)$ consists of harmonic orders which can be written as:

$$L(\theta) = L_0 + \sum_{n=1}^{\infty}(a_n\cos(n\theta) + b_n\sin(n\theta)) \quad (13)$$

in which, a_n and b_n are coefficients of fourier series. Due to the fact that first harmonic order of inductances participate in the torque production of VFRMs, neglecting the higher harmonic orders is reasonable in (12). Therefore, it is possible to calculate the mean torque by first harmonic order of inductances. Also, the value of torque ripple can be calculate by placing higher harmonic orders of inductances in (12).

IV. WFM, FEM, AND EXPERIMENTAL RESULTS

In order to validate the accuracy of the proposed WFM modelling of VFRM, a 6/7 VFRM which is proposed in [22] is selected as a case study. In this regard, results of the WFM, FEM, and experimental tests of the proposed VFRM, are going to be compared with each other in this section. It should be noted that the armature windings of the proposed design is concentrated with small end winding. Because the effect of end-winding is negligible, a 2-D study is employed. Table.1 shows the initial design of the proposed VFRM.

Table 1: Machine Specification

Parameter	Symbol	Value
Rotor diameter	D_r	46.4 mm
Stator outer diameter	D_o	90 mm
Stack length	L_s	25 mm
Air gap	g	0.5 mm
Stator pole arc	β_s	30^o
Rotor pole arc	β_r	23^o
Number of turn per field coil	N_{DC}	366
Number of turn per armature coil	N_a	183
Rated power	P	70 W
Rated speed	n	400 rpm
Number of phases	N_{ph}	3
DC bus voltage	V_{DC}	48V
Rotor pole number	P_r	7
Stator tooth number	T_s	6

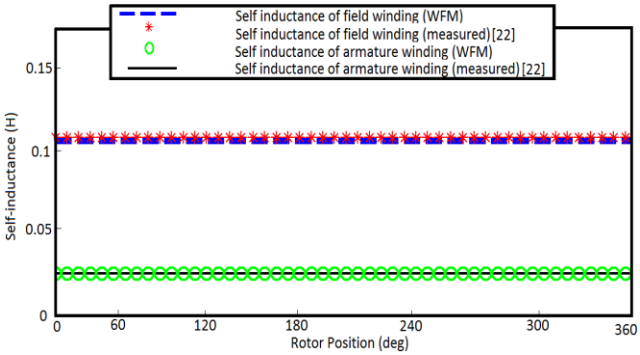

Fig. 11. Self-inductances of the proposed VFRM

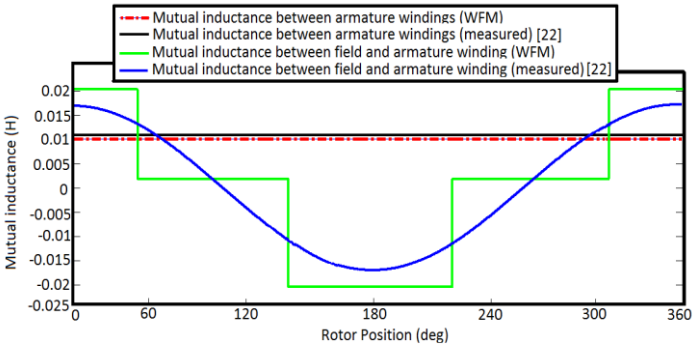

Fig. 12. Mutual-inductances of the proposed VFRM

The self-inductance of field and armature winding of VFRM are shown in Fig. 11. It can be concluded that the self-inductances are not participating in torque production due to their constant profile versus rotor rotation. Also, Fig. 12 shows the mutual-inductance profiles of windings. As it can be seen, the mutual-inductances between armature windings

is constant while the mutual-inductances between armature and field windings has a sinusoidal profile. Therefore, the variation of the mutual-inductances between armature and field windings, leads to the electromagnetic torque production. Fig. 13 shows the flux lines of the proposed VFRM, which is the result of FEM. Also, distribution of the magnetic flux density of the proposed VFRM is investigated in Fig. 14. It can be seen that alignment of rotor pole and stator tooth, leads to the maximum flux density which is 1.5T. The torque capability of VFRM is computed by WFM and the results are compared with the results of experimental test. Fig. 15 (a) and Fig. 15 (b) show the average torque which is computed by WFM and meaured by experimental tests in several q-axis currents with field current of 1 A and 2 A, respectively. It can be seen that the error of resultant average torque from WFM and experimental is less than 10 %, which proves the accuracy of the proposed WFM.

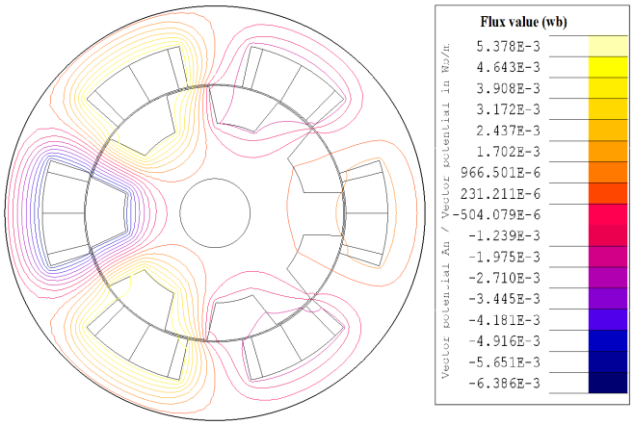

Fig. 13. Flux lines of the proposed 6/7 VFRM

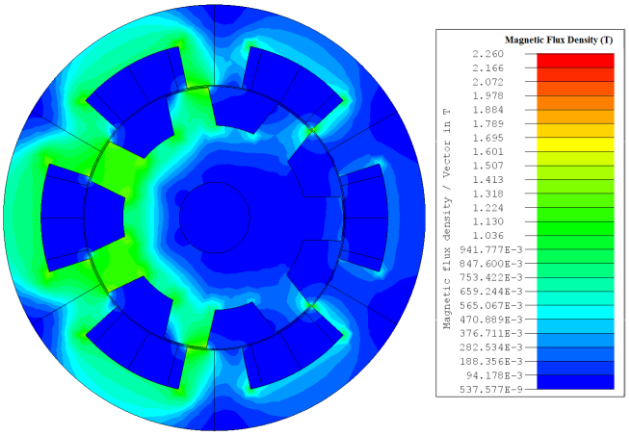

Fig. 14. Distribution of the magnetic flux density of the proposed 6/7 VFRM

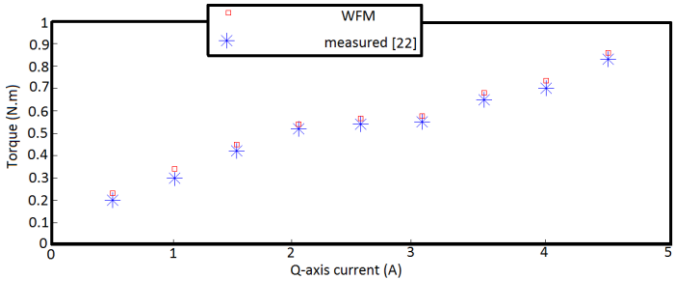

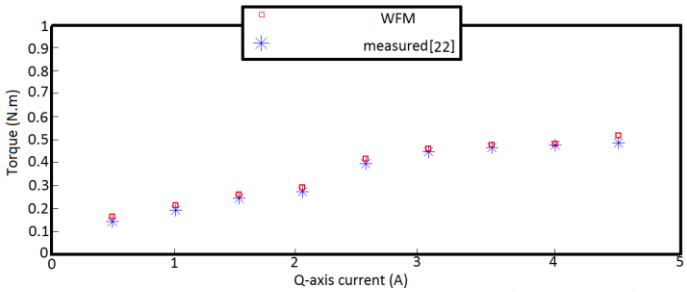

Fig. 15. Torque capability in several q-axis currents with field current of a)1 A; b) 2 A

V. Conclusion

In this paper, the VFRM which had 6 stator teeth and 7 rotor poles that proposed in [22], was modelled by WFM. The concept of VFRM and its performance were summarized. Also, the basic principal of WFM including computation of self-inductance, mutual-inductance, and torque were investigated. Due to the fact that the first harmonic order of mutual-inductances participated in torque production, the proposed WFM utilized a filter which divided the first and higher harmonic orders of inductances in order to compute average torque and torque ripple. The inductances which computed by WFM were compared with the results of experimental tests which were proposed in [22]. The results showed that the proposed WFM had a good accuracy in inductance and average torque computation. Therefore, it is a suitable and feasible alternative of FEM in analysis and optimization procedure of VFRMs because FEM takes long time for computation and optimization.

References

[1] B. Lee, Z. Q. Zhu, and L. Huang, "Investigation of Torque Production and Torque Ripple Reduction for Six-Stator/Seven-Rotor-Pole Variable Flux Reluctance Machines," *IEEE Transactions on Industry Applications*, vol. 55, no. 3, pp. 2510-2518, 2019.

[2] X. Liu, Z. Zhu, and D. Wu, "Evaluation of efficiency optimized variable flux reluctance machine for EVs/HEVs by comparing with interior PM machine," in *2014 17th International Conference on Electrical Machines and Systems (ICEMS)*, 2014, pp. 2648-2654: IEEE.

[3] C. Ditmanson, P. Hein, S. Kolb, J. Mölck, and S. Bernet, "A new modular flux-switching permanent-magnet drive for large wind turbines," *IEEE Transactions on Industry Applications*, vol. 50, no. 6, pp. 3787-3794, 2014.

[4] E. E. Mohamed, M. S. Saeed, and A. I. Ali, "Dual Three-Phase Partitioned Stator Flux-Switching PM Machine for Wind Generating Systems," in *2018 Twentieth International Middle East Power Systems Conference (MEPCON)*, 2018, pp. 992-997: IEEE.

[5] C. Yu and S. Niu, "Development of a magnetless flux switching machine for rooftop wind power generation," *IEEE Transactions on Energy Conversion*, vol. 30, no. 4, pp. 1703-1711, 2015.

[6] S. M. K. Sangdehi, S. E. Abdollahi, and S. A. Gholamian, "Analysis of a Novel Transverse Laminated Rotor Flux Switching Machine," *IEEE Transactions on Energy Conversion*, vol. 33, no. 3, pp. 1193-1202, 2018.

[7] A. S. Selema, D. S. Osheba, M. M. El-Shanawany, and S. M. Tahoun, "Design and Analysis of a Brushless Three Phase Flux Switching Generator for Aircraft Auxiliary Power Unit," in *2018 Twentieth International Middle East Power Systems Conference (MEPCON)*, 2018, pp. 198-202: IEEE.

[8] Y. Tang, J. J. Paulides, and E. A. Lomonova, "Automated design of dc-excited flux-switching in-wheel motor using magnetic equivalent circuits," in *2014 Ninth International Conference on Ecological Vehicles and Renewable Energies (EVER)*, 2014, pp. 1-10: IEEE.

[9] Y. Chen, Z. Q. Zhu, and D. Howe, "Three-Dimensional Lumped-Parameter Magnetic Circuit Analysis of Single-Phase Flux-Switching Permanent-Magnet Motor," *IEEE Transactions on Industry Applications*, vol. 44, no. 6, pp. 1701-1710, 2008.

[10] B. L. J. Gysen, E. Ilhan, K. J. Meessen, J. J. H. Paulides, and E. A. Lomonova, "Modeling of Flux Switching Permanent Magnet Machines With Fourier Analysis," *IEEE Transactions on Magnetics*, vol. 46, no. 6, pp. 1499-1502, 2010.

[11] J. Bao, S. R. Aleksandrov, B. L. Gysen, and E. A. Lomonova, "Analysis of variable flux reluctance machines using hybrid analytical modelling," in *2018 Thirteenth International Conference on Ecological Vehicles and Renewable Energies (EVER)*, 2018, pp. 1-7: IEEE.

[12] K. Ahmadian and A. Jalilian, "A new method in modeling of rotor bar skew effect in induction motor based on 2D-modified winding function method," in *2007 International Power Engineering Conference (IPEC 2007)*, 2007, pp. 630-635: IEEE.

[13] Y. Gao, R. Qu, and D. Li, "Improved hybrid method to calculate inductances of permanent magnet synchronous machines with skewed stators based on winding function theory," *Chinese Journal of Electrical Engineering*, vol. 2, no. 1, pp. 52-61, 2016.

[14] T. Lubin, T. Hamiti, H. Razik, and A. Rezzoug, "Comparison between finite-element analysis and winding function theory for inductances and torque calculation of a synchronous reluctance machine," *IEEE Transactions on Magnetics*, vol. 43, no. 8, pp. 3406-3410, 2007.

[15] R. Alipour-Sarabi, Z. Nasiri-Gheidari, F. Tootoonchian, and H. Oraee, "Improved Winding Proposal for Wound Rotor Resolver Using Genetic Algorithm and Winding Function Approach," *IEEE Transactions on Industrial Electronics*, vol. 66, no. 2, pp. 1325-1334, 2019.

[16] F. Boubakar, K. Abdellah, A. Mehdi, and A. Aissa, "Torque ripple reducing in SRM based on winding function theory and 3D Finite Element Methods," in *2015 4th International Conference on Electrical Engineering (ICEE)*, 2015, pp. 1-5: IEEE.

[17] I. Tabatabaei, J. Faiz, H. Lesani, and M. T. Nabavi-Razavi, "Modeling and Simulation of a Salient-Pole Synchronous Generator With Dynamic Eccentricity Using Modified Winding Function Theory," *IEEE Transactions on Magnetics*, vol. 40, no. 3, pp. 1550-1555, 2004.

[18] M. Jannati, T. Sutikno, N. R. N. Idris, and M. J. A. Aziz, "Modeling of Balanced and Unbalanced Three-Phase Induction Motor under Balanced and Unbalanced Supply Based on Winding Function Method," *International Journal of Electrical & Computer Engineering (2088-8708)*, vol. 5, no. 4, 2015.

[19] A. K. Ibrahim, M. I. Marei, H. El-Goharey, and S. A. Shehata, "Modeling of induction motor based on winding function theory to study motor under stator/rotor internal faults," in *14th Int. Middle East Power Systems Conference,(MEPCON'10), Cairo, Egypt*, 2010.

[20] M. Nourmohammadpour, M. Khalilzadeh, and K. Abbaszadeh, "Accurate modeling of switched reluctance motor by using improved winding function method," in *2014 22nd Iranian Conference on Electrical Engineering (ICEE)*, 2014, pp. 793-797: IEEE.

[21] J. P. Johnson, A. V. Rajarathnam, H. A. Toliyat, S. Gopalakrishnan, and B. Fahimi, "Torque optimization for a SRM using winding function theory with a gap-dividing surface," in *IAS'96. Conference Record of the 1996 IEEE Industry Applications Conference Thirty-First IAS Annual Meeting*, 1996, vol. 2, pp. 753-760: IEEE.

[22] X. Liu and Z. Q. Zhu, "Electromagnetic Performance of Novel Variable Flux Reluctance Machines With DC-Field Coil in Stator," *IEEE Transactions on Magnetics*, vol. 49, no. 6, pp. 3020-3028, 2013.